



Investigation on the feasibility of strain measurement by in situ neutron diffraction in the area of the weld pool during welding

R. Sharma^{a,*}, M. Hofmann^b, U. Reisgen^a

^a RWTH Aachen University, Welding and Joining Institute, Aachen, Pontstr. 49, 52062, Germany

^b Heinz Maier-Leibnitz Zentrum (MLZ), Technical University of Munich, Garching, Lichtenbergstrasse 1, 85748, Germany

Introduction

Residual stress formation in welding of metallic materials is one of the key influencing factors regarding the materials performance of welded components. Stress formation is bound to the thermal cycle of the welding process, which leads to a transient local change of the temperature dependent thermophysical and thermomechanical materials properties. Residual stresses build up in the material due to shrinkage constraints caused by geometry and clamping conditions.

Although residual stress formation is inherent to fusion welding, due to the inhomogeneous thermal field introduced by the moving heat source, the quantitative prediction of the stress field in welded components is still challenging. One reason for this is the complicated microstructural changes that occur in the weld metal and heat-affected zone during the welding thermal cycle. The occurrence of phase transformations further complicates accurate prediction. Furthermore specific thermophysical and thermomechanical materials data are difficult to determine experimentally. In addition, simplified material models are used for the analysis, which make the calculation numerically efficient, but at the same time introduce uncertainties.

The main physical processes leading to the formation of stresses and strains in the weld zone are known since long and have been outlined in [1].

A characteristic feature of fusion welding is the temporally and locally inhomogeneous temperature field. In the weld zone, the material is subject to intense heating and local melting. The yield strength drops as a result of the heating. In the area of the molten pool, tensile forces can only be absorbed at the level of the surface tension. Thermal expansion, in conjunction with strain restraint by the surrounding colder material, can lead to the buildup of compressive stresses. After solidification of the weld pool, thermal shrinkage leads to the formation of tensile stresses, which can be relieved to a lesser extent by plasticizing as the temperature drops due to the increasing yield point. In addition,

time-dependent deformation behavior also occurs in the high temperature range, which in the short-time range is determined in particular by dislocation movement. This results in stress relaxation. Solid state phase transformations further increase the complexity of the stress buildup during welding. The experimental determination of residual stresses in welded joints involves a great deal of effort. Furthermore, the quality of the results depends strongly on the boundary conditions of the sample (alloy, microstructure, analysis position) [2,3].

Although extensive research work has been done in the past to better understand the build-up of residual stress and distortion, it is still difficult to precisely predict the quantitative amount of stress and strain at a given location. For this purpose numerical welding simulation is used alternatively. The basic process of arc welding structural simulation starts with modelling a moving heat source. This is typically not done by calculating the physical phenomena which lead to heat evolution, but rather by an equivalent surrogate heat source. Here, the power density distribution is projected onto the melt pool geometry. A geometrical model of the part to be welded, the thermal and mechanical boundary conditions and the temperature dependent materials properties are used to simulate welding induced deformations and stresses. Therefore solid state mechanical models are needed, to represent the stress-strain relationship.

A simplified representation of the thermomechanical processes in the zone around the weld pool was given by Radaj (Fig. 1) [4]. The weld pool and the surrounding zone can be considered almost stress-free. At this point, surface tension and gravity primarily contribute to the balance of forces at the solidification line. Due to the progressive movement of the heat source, thermal expansion in front of the melt pool results in an area where compressive stresses prevail. Along the peak temperature curve, a change from compressive to tensile stress takes place.

An experimental validation of the model has hardly been possible so far, as measurement methods can only capture the strain state inside the material with difficulty. With the help of optical strain measurement

* Corresponding author.

E-mail address: sharma@isf.rwth-aachen.de (R. Sharma).

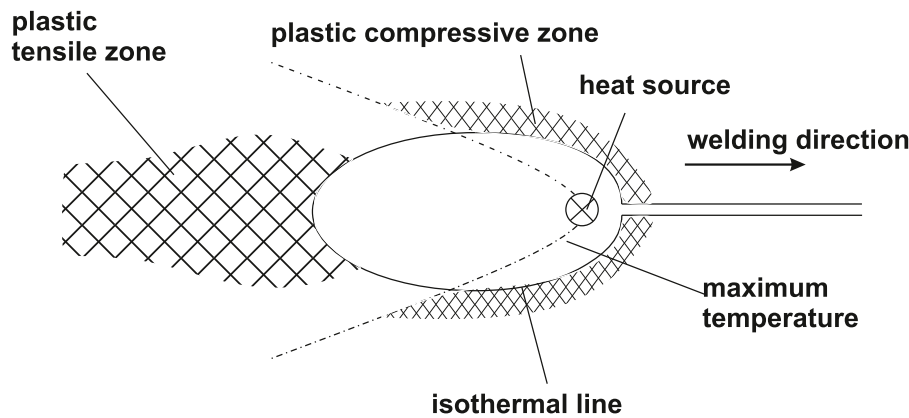


Fig. 1. Schematic top view of the thermomechanical behaviour of a joint weld zone between two plates, after [4].

Table 1

Chemical composition of the base metal (determined by spark optical emission spectroscopy).

	Si	Mn	Mg	Fe	Zn	Ni	Cu	Ti	Al
EN-AW1050	0,07	0,005	0,009	0,25	0,01	0,005	< 0,001	0,018	99,63

methods, indications of a corresponding zone distribution in the area around the weld pool could be obtained [5]. For thin plates, digital image correlation revealed more detailed information on the strain field in the weld zone [6] with a compressive strain zone in front of the weld pool. But only diffraction with neutron or synchrotron radiation has made it possible to take experimental measurements of the zone near the fusion line during welding in thicker material sections. Former investigations of diffraction strain measurement during welding mostly focused on phase transformation phenomena. [7–9].

At the same time, a precise knowledge of the prevailing thermo-mechanical boundary conditions is crucial for the calculation of residual stresses. Furthermore, the experimental determination of the strain field also allows the assessment of the risk of hot cracking phenomena. The formation of these material separations occurring at high temperatures between liquidus and solidus is closely linked to strain or strain rate in susceptible metallic materials [10]. It is therefore interesting to assess the transient strain field in the weld pool surrounding zone. The experimental determination of the strain field in the high temperature range below the sample surface during welding was the focus of the investigations described here. Essential here was the question whether such a transient determination of the strain field by neutron diffraction is feasible.

Due to the alignment of the diffractometer and the welding process, it was not possible to measure the strain in three independent spatial directions in the experiment, as this would have required changing the welding position between the tests. However, this would have significantly influenced the weld pool geometry. Thus, no complete specification of the stress tensor is possible on the basis of the present experiment. This represents a general difficulty of in-situ diffraction experiments during welding. Even the use of synchrotron radiation could only provide a solution if multiple detectors were available that could be freely arranged spatially.

Materials and methods

To investigate the strain field near the weld pool, welding tests were carried out on a neutron diffractometer, with the measurement taking place simultaneously with the welding movement. The base material used for the tests were cuboids made of commercially pure Aluminium alloy 1050 (EN 573-3 - EN-AW1050, Al99.5, Table 1), on which a blind bead was welded using the TIG process without the addition of filler

Table 2

Welding process conditions.

Electrode	Unthoriated, EN ISO 6848 WG, 3,2 mm
shielding gas	EN ISO 14175-11 (Ar 4.6), 12 l/min
contact tip to workpiece distance	2 mm
welding current	200 A
Welding voltage	17,5 V
welding speed	5 cm/min
Current form	AC
Energy input	42 kJ/cm
Filler wire	none
sample size (length x width x height)	200 × 100 × 30 mm ³

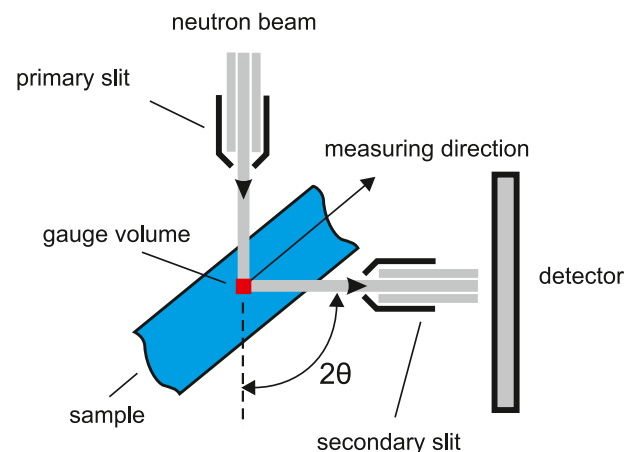


Fig. 2. Top view of the diffractometer setup.

metal. The boundary conditions are listed in Table 2. The welding process was carried out in flat position. The aim was to set up a quasi-stationary thermal field.

The investigations were carried out on the STRESS-SPEC diffractometer at the MLZ in Garching, Germany. The set-up of the instrument is described in detail in [11]. On the diffractometer table (Fig. 2), a sample was moved under the fixed welding torch with a linear table (Fig. 4). By adjusting the alignment of the entire unit relative to the beam slits, the measuring position of the neutron beam could be

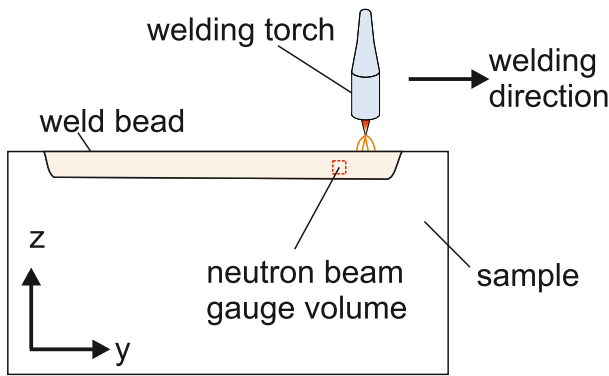


Fig. 3. Side view of the sample moving under the welding torch and the neutron beam.

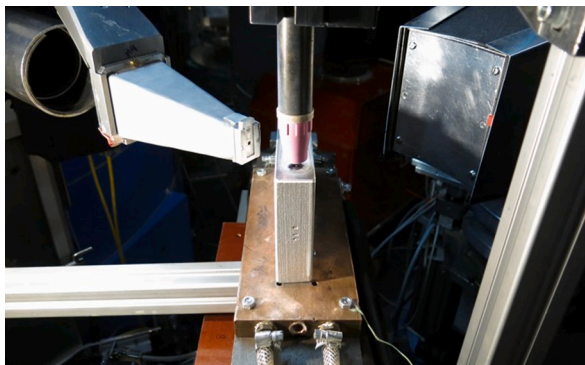


Fig. 4. Front view of the welding setup and sample mounted on the diffractometer.

Table 3
Parameters of the diffraction experiment.

monochromator wavelength	$\lambda = 1,55 \text{ \AA}$
slit size	$3 \times 3 \text{ mm}^2$
gauge volume	$3 \times 3 \times 2 \text{ mm}^3$
evaluated diffraction reflex	311
exposure time	120 s

determined. Measurements were taken in a grid relative to the heat source. Here, measurements were taken in the welding direction in front of the electrode (20 mm, 10 mm, 7 mm), and after the electrode (4 mm, 10 mm, 20 mm) along the centre axis of the specimen. The readings were taken at three depths below the surface of the specimen (2 mm, 5 mm and 8 mm). A whole sample was welded for each measuring point, in order to reach the required measuring time to achieve a stable diffraction reflex of approx. 30 s. Due to the high reproducibility of the weld pool geometry and the thermal field when using the TIG process without the addition of filler metal, the application of this method is possible. Fig. 3 shows a sample on the base plate, which was cooled down to room temperature by liquid cooling between the tests. This allowed the thermal boundary conditions of each test to be kept constant and the waiting time between tests to be shortened. Each measurement was repeated three times and the mean value was used for the further calculation of the strain field. The basic diffraction parameters are given in Table 3.

The foundation of the calculation of elastic strains on the basis of neutron diffraction is the application of Bragg's equation (Eq. 1)

$$d_{311} = \frac{\lambda}{2\sin\Theta} \tag{Equation 1}$$

Here, d_{311} is the lattice plane spacing for the (311) plane, λ the wavelength of the neutron beam and Θ the diffraction angle. The measurement volume is defined by primary and secondary slits, allowing a targeted localisation of the strain measurement in the volume of the specimen to be achieved. The alignment of the neutron beam was chosen in the experiment so that measurement in the main strain direction (parallel to the welding direction) of the specimen is possible.

The evaluation of the recorded diffraction data was carried out with the software Steca [12,13]. This was used to reduce the background and to perform a peak fit via a Gaussian function. The efficiency of the detector was calibrated via a correction measurement of a vanadium sample.

To evaluate the mechanical strain based on the neutron diffraction data, it is necessary to separate the thermal strain component from the elastic strain. This requires exact knowledge of the temperature field. The sample was observed laterally with a thermal camera during the tests. To calibrate the surface temperature, a type K thermocouple was attached to the surface and a coating of boron nitride suspension was applied to adjust the emissivity.

The determination of the thermal expansion of the sample material was carried out via a dilatometer experiment of a sample of the same material in a special vacuum furnace on the diffractometer and the (311)

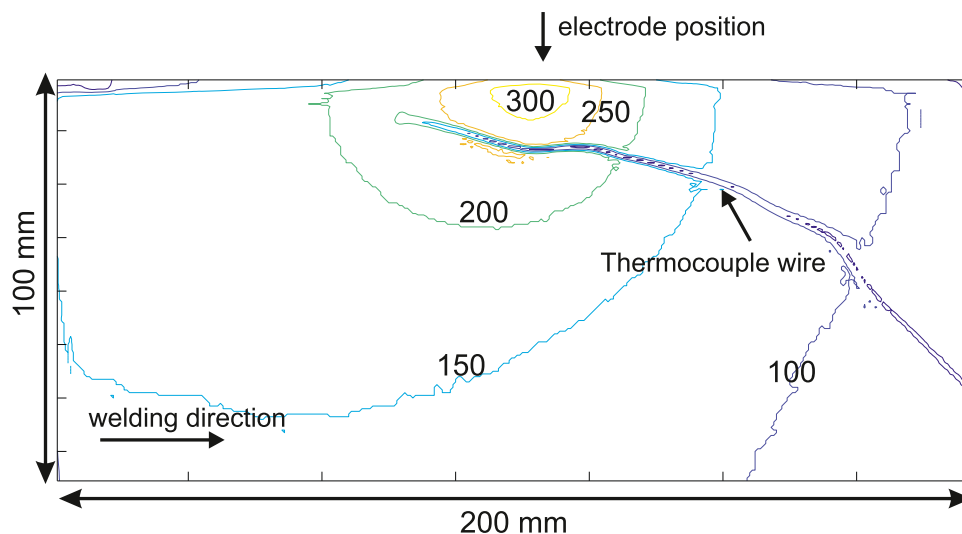


Fig. 5. Thermal field on the side surface of the sample, measured by thermal imaging, Temperatures given in °C.

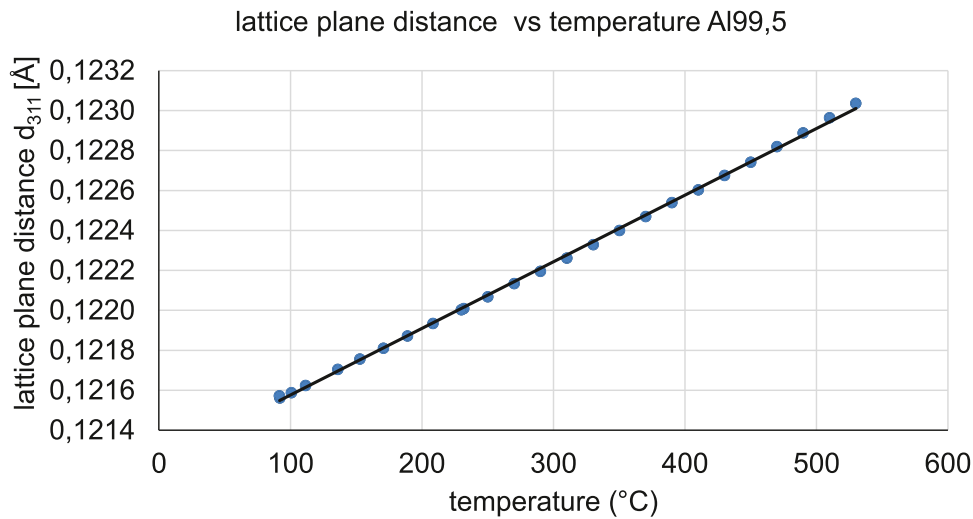


Fig. 6. Thermal expansion curve of EN-AW1050 sample measured on STRESS-SPEC during the furnace experiment. The (311) lattice spacing was measured.

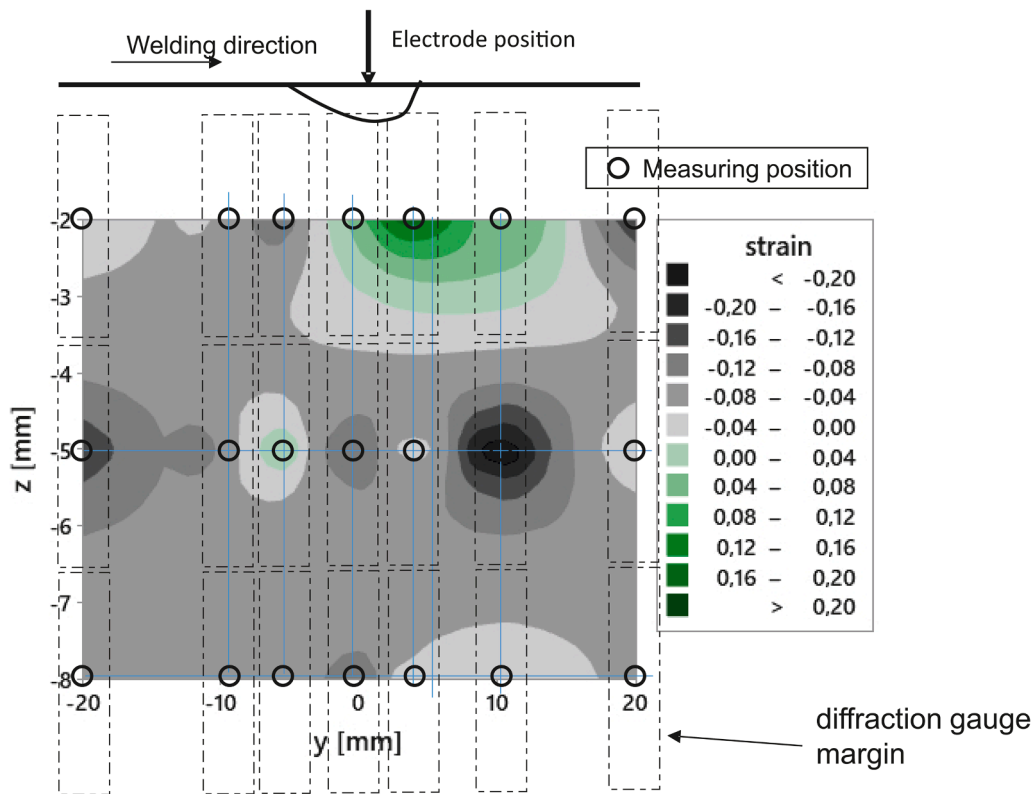


Fig. 7. Strain field below the weld pool during welding, side view of the centre plane.

lattice plane spacing was measured in the temperature range considered.

Results

The isothermal field based on the thermographic images on the side surface of the sample is shown in Fig. 5. Some part of the image is affected by a thermocouple wire for point comparison measurement. Due to the selected diffraction measurement volume of $3 \times 3 \times 2 \text{ mm}^3$, only the isotherms at a distance of 50 K were determined here. On this basis, a numerical welding simulation was calibrated with the welding structure simulation package Simufact.Welding 2020. The procedure is described in more detail in [8]. This step was necessary since the

experimental temperature measurement only determined the temperature field at the surface. With the help of the simulated temperature field, the average temperature of the diffraction gauge volume could then be determined.

By subtracting the reference value for the lattice plane spacing at the average temperature of the measuring volume, the mechanically induced part of the strain vector can be determined. The curve for the reference value determined in the furnace experiment is shown in Fig. 6.

Based on the temperature determination of the measurement gauge and the temperature dependent thermal strain subtraction, the mechanical strain field parallel to the welding direction was determined (Fig. 7). A section plane in the centre of the specimen was chosen.

Table 4

Longitudinal Stress (in welding direction y), measured along the centreline of the sample, 5 mm below the top surface.

sample length position [mm]	80	100	120
Stress [MPa]	19,7±4,0	28,3±3,0	24,8±3,2

The image section shown starts 2 mm below the top of the sample (position $z = -2$ mm) because the measuring volume must be completely inside the sample for a valid measurement. It can be ruled out that the area of highest tensile strain lies in front of the melt pool. This is where a noticeable elongation takes place. Due to the large temperature gradients and the error caused by this, no other significant areas in the measuring range can be identified. Also below the weld pool, there is a clear elastic elongation. If one takes into account that the zone of highest temperature lies directly below the weld pool, the maximum reduction of the yield strength starts here. This results in a relaxation of the stress field due to plastic deformation. Taking into account the high temperature, it should be noted that a time-dependent strain behaviour must be assigned to the material, which, however, cannot be resolved with the method used here. At high temperatures stress relaxation happens in the vicinity of the weld pool due to viscoplastic behaviour and creep phenomena, depending on temperature gradients within the gauge volume, thermal cycle and the specific material involved [14]. Only the elastic part is visible here, even if additional plastic/viscoplastic parts contribute to the macroscopic total strain. After solidification of the weld metal, the material can again absorb tensile forces during cooling behind the weld pool and elastic elongation occurs due to hindered thermal shrinkage. The results thus support theoretical considerations by Radaj and others on strain distribution in the weld zone during welding with a moving heat source [4,5], schematically summarized in Fig. 1.

At the same time, the spatial resolution of the method does not allow an accurate statement on zones of small strains. In particular, a smaller gauge volume is necessary for the investigation of the critical boundary conditions for the formation of hot cracks in combination with even shorter measurement times.

For in-situ investigations with neutron diffraction, it is important to assure the uniformity of the quasistationary conditions. In the present experiment, this was verified via an ex-situ measurement of the residual stress at different points over the entire sample length (Table 4). For the given sample geometry, the stress level can be considered fairly uniform at the measurements locations.

Conclusion

Decisive for the quality of in-situ experiments with neutron scattering is the time scale considered. The long necessary measurement times in the order of minutes for the materials, gauge volumes and beam paths concerned here only permit an application for quasi-stationary conditions. The verification of these quasi-stationary conditions is therefore of crucial importance

The results clarify that in-situ neutron diffraction can be used to characterise the strain field near the molten pool and thereby resolve areas with tensile strains in the cooling zone. In particular, it was possible to support a widespread model conception of the thermo-mechanical constitution of the area near the melt pool. On the one hand, this is helpful for the validation of thermomechanical simulations of welding processes, as well as for the detection of process conditions in

which there is a risk of hot cracking. However, an increased spatial and temporal resolution would be helpful for this, as temperature gradients of several 100 K can sometimes occur within the measurement volume. In future, investigations will therefore be carried out using high-energy X-rays, as this appears to provide a higher resolution and much shorter measurement times.

Declaration of Competing Interest

The authors declare that they have no known competing financial interests or personal relationships that could have appeared to influence the work reported in this paper.

Acknowledgement

All presented investigations were conducted in the context of the Collaborative Research Centre SFB1120 "Precision Melt Engineering" at RWTH Aachen University and funded by the German Research Foundation (DFG). For the sponsorship and the support, we wish to express our sincere gratitude. (Project ID 236616214) This work is based upon experiments performed at the STRESS-SPEC instrument operated by Hereon at the Heinz Maier-Leibnitz Zentrum (MLZ), Garching, Germany.

References

- [1] Y Ueda, T. Yamakawa, Analysis of Thermal Elastic-Plastic Behavior of Metals during Welding by Finite Element Method, *J. Jap. Weld. Soc.* 42 (6) (1973) 567–577, <https://doi.org/10.2207/qjwsl1943.42.567>.
- [2] U Dilthey, U Reisgen, M. Kretschmer, Comparison of FEM simulations to measurements of residual stresses for the example of a welded plate: a state-of-the-art report, *Modelling Simul. Mater. Sci. Eng.* 8 (6) (2000) 911–926, <https://doi.org/10.1088/0965-0393/8/6/311>.
- [3] K Bobzin, W Wietheger, MA Knoch, A Schacht, U Reisgen, R Sharma, et al., Comparison of Residual Stress Measurements Conducted by X-ray Stress Analysis and Incremental Hole Drilling Method, *J. Therm. Spray. Tech.* 29 (6) (2020) 1218–1228, <https://doi.org/10.1007/s11666-020-01056-z>.
- [4] D. Radaj, Heat effects of welding: Temperature field, residual stress, distortion; with 265 figures, Springer, Berlin, 1992.
- [5] T. Zacharia, Dynamic stresses in weld metal hot cracking, *Weld. J.* (7) (1994) 164s–172s.
- [6] M Pliazhuk, C Reyes, M Martinez, J Goldak, H Nimrouzi, DK Aidun, Situ Monitoring of Transient Strain Formation in Vertical Welds, *Weld. J.* 98 (9) (2019) 251s–262s.
- [7] J Dixneit, F Vollert, A Kromm, J Gibmeier, A Hannemann, T Fischer, et al., In situ analysis of the strain evolution during welding using low transformation temperature filler materials, *Sci. Technol. Weld. J.* 58 (3) (2018) 1–13, <https://doi.org/10.1080/13621718.2018.1525150>.
- [8] R Sharma, U Reisgen, M. Hofmann, Comparison of Submerged Arc Welding Process Modification Influence on Thermal Strain by in-situ Neutron Diffraction, in: TM Holden, O Muránsky, L Edwards (Eds.), *Residual Stresses 2016*, Materials Research Forum LLC, 2017, pp. 533–538.
- [9] J Gibmeier, E Held, J Altenkirch, A Kromm, T Kannengiesser, T. Buslaps, Real time monitoring of phase transformation and strain evolution in LTT weld filler material using EDXRD, *J. Mater. Proc. Technol.* 214 (11) (2014) 2739–2747, <https://doi.org/10.1016/j.jmatprotec.2014.06.008>.
- [10] CE. Cross, On the Origin of Weld Solidification Cracking, in: T Böllinghaus, H Herold (Eds.), *Hot cracking phenomena in welds: International workshop; March 2004*, Springer, Berlin, 2005, pp. 3–18.
- [11] M Hofmann, W Gan, J. Rebelo-Kornmeier, STRESS-SPEC: Materials science diffractometer, *JLSRF 1* (2015), <https://doi.org/10.17815/jlsrf-1-25>.
- [12] C Randau, U Garbe, H-G. Brokmeier, StressTextureCalculator a software tool to extract texture, strain and microstructure information from area-detector measurements, *J. Appl. Crystallogr.* 44 (3) (2011) 641–646, <https://doi.org/10.1107/S0021889811012064>.
- [13] RE Brydon, J Burlle, J Coenen, W Gan, M Hofmann, J Katter, et al., *steca: Stress and texture calculator*, MLZ, 2021.
- [14] UEDA, Yukio, FUKUDA, Keiji. Application of Finite Element Method for Analysis on Process of Stress Relief Annealing. *Trans. Jap. Weld. Soc.* 8(1):19–25.